

CLIMB-3D: Continual Learning for Imbalanced 3D Instance Segmentation

Vishal Thengane^{1*}  Jean Lahoud² Hisham Cholakkal² Rao Muhammad Anwer²
 Lu Yin¹ Xiatian Zhu¹ Salman Khan^{2,3}
¹University of Surrey, United Kingdom
²Mohamed bin Zayed University of Artificial Intelligence, UAE
³Australian National University, Australia
 v.thengane@surrey.ac.uk

Abstract

While 3D instance segmentation (3DIS) has advanced significantly, existing methods typically assume that all object classes are known in advance and are uniformly distributed. However, this assumption is unrealistic in dynamic, real-world environments where new classes emerge gradually and exhibit natural imbalance. Although some approaches have addressed class emergence, they often overlook class imbalance, resulting in suboptimal performance – particularly on rare categories. To tackle this challenge, we propose **CLIMB-3D**, a unified framework for **CLass-incremental IMbalance-aware 3DIS**. Building upon established exemplar replay (ER) strategies, we show that ER alone is insufficient to achieve robust performance under constrained memory conditions. To mitigate this, we introduce a novel pseudo-label generator (PLG) that extends supervision to previously learned categories by leveraging predictions from a frozen prior model. Despite its promise, PLG tends to bias towards frequent classes. Therefore, we propose a class-balanced re-weighting (CBR) scheme, that estimates object frequencies from pseudo-labels and dynamically adjusts training bias – without requiring access to past data. We design and evaluate three incremental scenarios for 3DIS on the challenging ScanNet200 dataset, and additionally on semantic segmentation on ScanNetV2. Our approach achieves state-of-the-art results, surpassing prior work by up to 16.76% mAP for instance segmentation and approximately 30% mIoU for semantic segmentation, demonstrating strong generalization across both frequent and rare classes.

1. Introduction

3D instance segmentation (3DIS) is an essential task in computer vision with widespread applications in graphics,

robotics, and augmented reality [2, 31]. It involves identifying and segmenting individual objects in 3D space, enabling precise object boundaries and class labels that enhance scene understanding and perception in dynamic environments.

In recent years, a variety of methods for 3DIS have been proposed, including top-down [23, 53, 59], bottom-up [21, 56], and transformer-based approaches [46]. These methods have demonstrated strong performance under the traditional setting, which assumes that all object classes are available and well-balanced during training. However, these assumptions limit their applicability in real world settings, where new categories gradually emerge over time, often exhibiting natural class imbalance.

These limitations in current 3DIS methods underscore the need for a *Class-Incremental Learning* (CIL) [14, 42] framework capable of learning new categories as they appear, while maintaining accuracy on previously learned classes – especially rare ones, which are more susceptible to without catastrophic forgetting [39]. Unfortunately, most existing research in CIL has focused on the 2D domain for image classification [1, 33, 42, 47], with limited extensions to object detection [25, 37, 48] and semantic segmentation [4, 5, 16]. Extensions to 3D point clouds remain limited, with most work focusing on object-level classification rather than scene-level segmentation [11, 15, 36]. Recent works on scene-level class-incremental 3DIS (CI-3DIS) [2] and class-incremental semantic segmentation (CI-3DSS) [57] show promise, but typically rely on large exemplar buffers [43]. Moreover, they typically overlook class imbalance, limiting real-world applicability.

To address this, we propose **CLIMB-3D**, a unified framework for **CLass-incremental IMbalance-aware 3DIS** that jointly tackles catastrophic forgetting and class imbalance. The framework begins with Exemplar Replay (ER), storing a small number of samples from past classes for later replay. However, this alone does not yield promising results under the strict memory constraints needed CI-3DIS. To ad-

*Work done during the time at MBZ University of AI, UAE

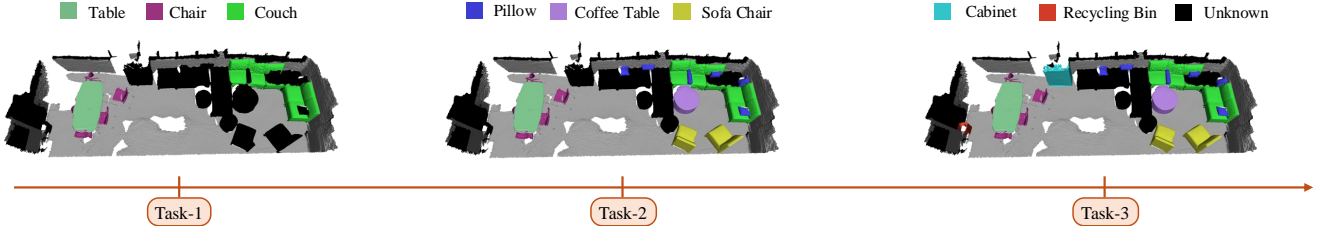


Figure 1. Overview of the CI-3DIS setting: new classes are introduced incrementally as tasks progress. After each task, the model must recognize both previously learned and newly added classes. For instance, at Task 2, classes like Pillow, Coffee Table, and Sofa Chair are introduced, while the model retains the ability to detect earlier classes such as Table, Chair, and Couch.

dress this, we introduce a Pseudo-Label Generator (PLG), which uses a frozen previous task model to generate supervision for earlier classes. However, we observed that, PLG tends to favour frequent classes while ignoring under-represented ones. To mitigate this, we propose a Class-Balanced Re-weighting (CBR), which estimates class frequencies from the pseudo-labels to enhance the learning of rare classes without accessing past data. Together, these components form a practical and effective solution for real-world 3DIS.

To evaluate **CLIMB-3D** in a realistic incremental setup, we design three benchmark scenarios using the ScanNet200 [44] dataset, which contains 200 classes with a natural long-tail distribution. These scenarios simulate real-world conditions where new classes gradually emerge, following inherently imbalanced distributions. Specifically, new classes appear in groups based on one of three criteria: (A) object frequency, (B) semantic similarity, or (C) random grouping without a specific pattern. Our experiments on these scenarios for incremental 3DIS show that **CLIMB-3D** effectively mitigates forgetting of previous tasks while improving performance across both frequent and rare classes, delivering consistent gains over prior methods.

In summary, our contributions are threefold: (i) We introduce a novel problem setting of imbalanced class-incremental 3DIS, along with a simple and effective method to mitigate catastrophic forgetting and ensure balanced learning; (ii) We establish three benchmark scenarios that realistically model continuous object emergence with natural class imbalance; and (iii) We validate our framework’s effectiveness, achieving SOTA results with improvements up to 16.76% mAP over existing baselines¹.

2. Related Work

This section reviews the current literature on 3D instance segmentation and incremental learning methods, including the limited work addressing incremental learning for 3D scene-level tasks.

¹Code will be available at: <https://github.com/vgthengane/CLIMB3D>

2.1. 3D Instance Segmentation

Various approaches have been proposed for 3D instance segmentation. One common approach adopts a bottom-up pipeline, in which an embedding in the latent space is learned to facilitate the clustering of object points [7, 18, 19, 24, 30, 34, 53, 59]. These methods are also known as grouping-based or clustering-based methods. Other methods use a top-down approach, also known as proposal-based methods, where 3D bounding boxes are first detected, then the object region is segmented within the box [17, 21, 35, 56, 58]. Recently, the transformer architecture [52] has also been used for the task of 3D instance segmentation [46, 51], motivated by work in 2D [8, 9]. While these methods propose various models for improving the quality of the object segments, they rely on the availability of annotations for all object categories. On the other hand, we target learning in a progressive manner, in which new semantic annotation is provided and past data is inaccessible.

In order to reduce the annotation cost for 3D instance segmentation, various methods propose weakly supervised alternatives to methods that use dense annotations [10, 22, 55]. While these methods improve the ability to learn from a small set of annotated examples, they rely on a fixed set of semantic labels, so they are prone to catastrophic forgetting in an incremental setting.

2.2. Incremental Learning

Incremental, lifelong, or continual learning methods aim to train a machine learning model sequentially to avoid “catastrophic forgetting” which is caused by training the model on a set of data and later training on another set of data. There are several methods have been proposed for this paradigm, these methods can be divided into three categories: (i) Model Regularization [1, 28, 33] methods limit the plasticity of model parameters to avoid catastrophic forgetting of previous tasks. These methods include weight regularization such as EWC [47] and function regularization such as knowledge distillation [20]. (ii) Exemplar replay approaches either create a subset of the past task data or generate samples using generative models to avoid pri-

vacy concerns and save those in memory to replay while learning new tasks. This method is effective in more challenging settings and datasets [3, 6, 26, 42]. (iii) Dynamic network expansion-based method learns a new task by either dynamically expanding the model [32, 45, 60] or by creating a subset of the model [27, 41, 54, 60] to learn to cater for a new task.

Recent approaches to 3D class-incremental segmentation, such as [57] and [50], have made some initial contributions. However, these methods often fall short in performance as they do not leverage state-of-the-art 3D segmentation models and are primarily focused on semantic segmentation, while our work emphasizes object-level instance segmentation. Kontogianni et al. [29] propose a general online continual learning framework and evaluate it on 3D dataset segmentation. Similarly, [2] addresses the open-world 3D incremental learning problem but relies heavily on an extensive memory buffer. In contrast, our work introduces a dedicated continual learning framework for 3D instance segmentation, with a focus on effective knowledge transfer from previous tasks, while also accounting for the challenges posed by infrequent class occurrences.

3. Methodology

3.1. Problem Formulation

3DIS. The objective of this task is to detect and segment each object instance within a given point cloud. Formally, the training dataset is denoted by $\mathcal{D} = \{(\mathbf{P}_i, \mathbf{Y}_i)\}_{i=1}^N$, where N is the number of training samples. Each input $\mathbf{P}_i \in \mathbb{R}^{M \times 6}$ is a colored point cloud consisting of M points, where each point is represented by its 3D coordinates and RGB values. The corresponding annotation $\mathbf{Y}_i = \{(m_{i,j}, c_{i,j})\}_{j=1}^{J_i}$ contains J_i object instances, where $m_{i,j} \in \{0, 1\}^M$ is a binary mask indicating the points belonging to the j -th instance, and $c_{i,j} \in \mathcal{C} = \{1, \dots, C\}$ is the semantic class label of that instance. Given \mathbf{P}_i , the model Φ predicts instance-level outputs $\hat{\mathbf{Y}}_i = \{(\hat{m}_{i,j}, \hat{c}_{i,j})\}_{j=1}^{\hat{J}_i}$, where $\hat{m}_{i,j}$ and $\hat{c}_{i,j}$ denote the predicted mask and category label for the j -th instance, respectively. The number of predicted instances \hat{J}_i varies depending on the model’s inference. The model is optimized using below objective:

$$\mathcal{L}_{\text{3DIS}}(\mathcal{D}; \Phi) = \frac{1}{|\mathcal{D}|} \sum_{(\mathbf{P}, \mathbf{Y}) \in \mathcal{D}} \frac{1}{|\mathbf{Y}|} \sum_{(m_j, c_j) \in \mathbf{Y}} (\mathcal{L}_{\text{mask}}(m_j, \hat{m}_j) + \lambda \cdot \mathcal{L}_{\text{cls}}(c_j, \hat{c}_j)) \quad (1)$$

where \mathcal{L}_{cls} and $\mathcal{L}_{\text{mask}}$ are the average classification and mask losses over all instances, and λ controls their trade-off.

CI-3DIS. Unlike conventional 3DIS, CI-3DIS involves sequential learning, where object categories are introduced

incrementally over T training tasks. Each task t introduces a disjoint set of classes \mathcal{C}^t , with $\mathcal{C} = \bigcup_{t=1}^T \mathcal{C}^t$ and $\mathcal{C}^t \cap \mathcal{C}^{t'} = \emptyset$ for $t \neq t'$. At each task t , the model receives a dataset $\mathcal{D}^t = \{(\mathbf{P}_i, \mathbf{Y}_i^t)\}_{i=1}^N$, where each coloured point cloud $\mathbf{P}_i \in \mathbb{R}^{M \times 6}$ contains M points, and the corresponding annotation $\mathbf{Y}_i^t = \{(m_{i,j}^t, c_{i,j}^t)\}_{j=1}^{J_i^t}$ includes instance masks $m_{i,j}^t \in \{0, 1\}^M$ and semantic labels $c_{i,j}^t \in \mathcal{C}^t$. The model Φ^t , initialized from Φ^{t-1} , is trained on \mathcal{D}^t to predict instance-level outputs $\hat{\mathbf{Y}}_i^t = \{(\hat{m}_{i,j}^t, \hat{c}_{i,j}^t)\}_{j=1}^{\hat{J}_i^t}$, where each predicted class label $\hat{c}_{i,j}^t$ belongs to the cumulative set of all classes observed so far: $\bigcup_{k=1}^t \mathcal{C}^k$. The optimisation objective for the CI-3DIS setting is defined as:

$$\mathcal{L}_{\text{CI-3DIS}}(\mathcal{D}^t; \Phi^t) = \frac{1}{|\mathcal{D}^t|} \sum_{(\mathbf{P}, \mathbf{Y}^t) \in \mathcal{D}^t} \frac{1}{|\mathbf{Y}^t|} \sum_{(m_j^t, c_j^t) \in \mathbf{Y}^t} (\mathcal{L}_{\text{mask}}(m_j^t, \hat{m}_j^t) + \lambda \cdot \mathcal{L}_{\text{cls}}(c_j^t, \hat{c}_j^t)). \quad (2)$$

The key challenge in this setup is to learn new classes without forgetting those encountered in previous tasks, despite limited supervision and the absence of past labels.

3.2. Method: CLIMB-3D

Overview. As illustrated in Fig. 2 and introduced in Sec. 3.1, the proposed framework for CI-3DIS follows a *phase-wise* training strategy. In each phase, the model is exposed to a carefully selected subset of the dataset, designed to simulate real-world scenarios discussed in Sec. 3.3. Naïvely training on such phased data leads to *catastrophic forgetting* [39], where the model forgets previously acquired knowledge when learning new tasks. To address this, we first incorporate *Exemplar Replay (ER)* [3], inspired by 2D [1, 33, 42] and 3D [2] incremental setting, to mitigate forgetting by storing a small set of representative samples from earlier phases. However, ER alone is insufficient for achieving robust performance. We therefore introduce two additional components: a *Pseudo-Label Generator (PLG)*, which leverages a frozen model to generate supervision signals for previously seen classes, and a *Class-Balanced Reweighting (CBR)* module that compensates for class imbalance across phases. Each of these components is described in detail below².

Exemplar Replay (ER). Inspired by Buzzega et al. [3], ER addresses the issue of catastrophic forgetting by allowing the model to retain a small portion of data from earlier phases. At phase t , the model is trained not only on the current task data \mathcal{D}^t but also on a set of exemplars $\mathcal{E}^{1:t-1}$ collected from previous phases. These exemplars are accumulated incrementally, where $\mathcal{E}^{1:t-1} = \mathcal{E}^1 \cup \dots \cup \mathcal{E}^{t-1}$, and

²For clarity, modifications introduced by each component – ER, PLG, and CBR – are highlighted in green, blue, and red, respectively.

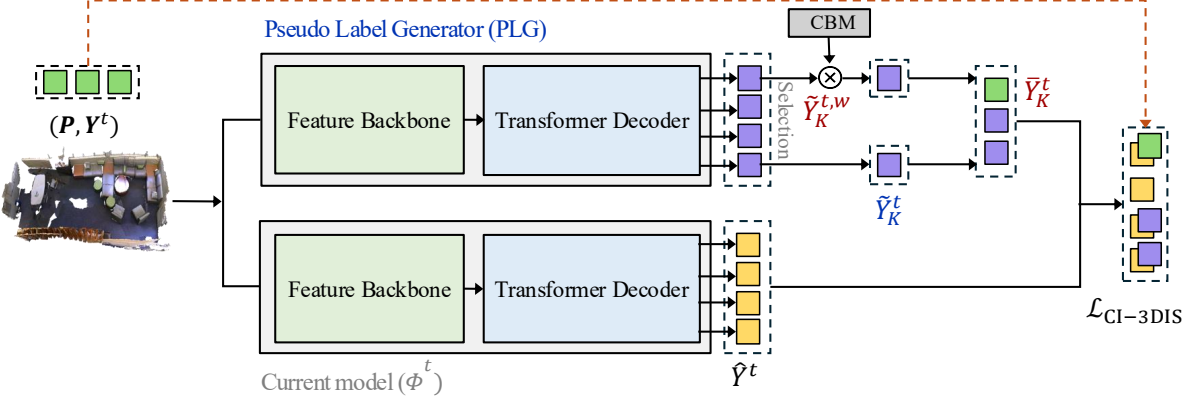


Figure 2. Overview of **CLIMB-3D** for CI-3DIS. The model incrementally learns new classes in sequential phases using ER to mitigate forgetting, a PLG for supervision on old classes, and CBR to handle class imbalance.

\mathcal{E}^t denotes the exemplar subset stored after phase t , with $|\mathcal{E}^t|$ as the exemplar replay size. We define the combined replay dataset as: $\mathcal{D}_{\text{ER}}^t = \mathcal{D}^t \cup \mathcal{E}^{1:t-1}$. Epoch training proceeds in two stages: first on the current data \mathcal{D}^t , followed by replay using $\mathcal{E}^{1:t-1}$. The updated objective function for CI-3DIS, based on ??, becomes:

$$\mathcal{L}_{\text{CI-3DIS}}(\mathcal{D}_{\text{ER}}^t; \Phi^t) = \frac{1}{|\mathcal{D}_{\text{ER}}^t|} \sum_{(\mathbf{P}, \mathbf{Y}^t) \in \mathcal{D}_{\text{ER}}^t} \frac{1}{|\mathbf{Y}^t|} \sum_{(m_j^t, c_j^t) \in \mathbf{Y}^t} (\mathcal{L}_{\text{mask}}(m_j^t, \hat{m}_j^t) + \lambda \cdot \mathcal{L}_{\text{cls}}(c_j^t, \hat{c}_j^t)). \quad (3)$$

While previous CI-3DIS approaches use large exemplar sets to mitigate forgetting [2], such strategies become impractical under memory constraints. Consequently, although exemplar replay (ER) aids knowledge retention, it alone proves insufficient for robust performance with a limited exemplar budget. We therefore propose PLG and CBR to better preserve past representations and enhance generalisation across phases.

Pseudo-Label Generator (PLG). In the CI-3DIS setting, at phase t (for $t > 1$), although we no longer have access to the ground-truth labels for previously seen classes, the model from the previous phase, Φ^{t-1} , remains available and retains knowledge acquired from past tasks. We use this model to generate pseudo-labels for previous classes, thereby providing approximate past supervision during training. This allows the current model Φ^t to retain past knowledge and reduces forgetting, even without access to original annotations.

Given a point cloud and label pair $(\mathbf{P}, \mathbf{Y}^t)$ from \mathcal{D}^t , the previous model Φ^{t-1} generates pseudo-labels for the previously learned classes as $\tilde{\mathbf{Y}}^{1:t-1} = \Phi^{t-1}(\mathbf{P})$, which we denote as $\tilde{\mathbf{Y}}^t$ for brevity. However, we observe that using all predictions from Φ^{t-1} introduces noisy or incorrect labels, which degrade overall performance. To mitigate this,

we select the top- K most confident instance predictions, denoted as $\tilde{\mathbf{Y}}_K^t$, and concatenate them with the ground-truth labels of the current task to obtain the supervision set: $\bar{\mathbf{Y}}^t = \mathbf{Y}^t \parallel \tilde{\mathbf{Y}}_K^t$. At the end, Using this supervision set, the model is optimized via the following updated objective:

$$\mathcal{L}_{\text{CI-3DIS}}(\mathcal{D}_{\text{ER}}^t; \Phi^t) = \frac{1}{|\mathcal{D}_{\text{ER}}^t|} \sum_{(\mathbf{P}, \mathbf{Y}^t) \in \mathcal{D}_{\text{ER}}^t} \frac{1}{|\bar{\mathbf{Y}}^t|} \sum_{(\bar{m}_j^t, \bar{c}_j^t) \in \bar{\mathbf{Y}}^t} (\mathcal{L}_{\text{mask}}(\bar{m}_j^t, \hat{m}_j^t) + \lambda \cdot \mathcal{L}_{\text{cls}}(\bar{c}_j^t, \hat{c}_j^t)), \quad (4)$$

where the loss is computed over both the current task's ground-truth labels and the top- K confident pseudo-labels from previous phases, enabling the model to retain prior knowledge while adapting to new classes.

Class-Balanced Re-weighting (CBR). While ER and PLG contribute to preserving prior knowledge, we observe that the model's predictions are biased toward frequently occurring classes, leading to forgetting of rare categories. This issue is further reinforced by the top- K pseudo-labels selected by PLG, which predominantly represent dominant classes in the data. To alleviate this issue, we introduce a *Class-Balanced Re-weighting* (CBR) scheme that adjusts for class imbalance based on frequency of object occurrence. However, at task t , we only have access to the dataset \mathcal{D}^t and its corresponding label distribution $p^t(c)$ over classes $c \in \mathcal{C}^t$. The datasets and class distributions from previous tasks $\{\mathcal{D}^i, p^i(c)\}_{i=1}^{t-1}$ are no longer accessible – making it challenging to directly account for class imbalance across all seen tasks. Therefore, we propose to leverage the pseudo-label predictions of the frozen model Φ^{t-1} as a proxy for the class distribution across previously learned categories.

During each training iteration, we apply the previous model Φ^{t-1} to the current input point cloud \mathbf{P} to generate pseudo-labels $\tilde{\mathbf{Y}}^t$, from which we accumulate class-

wise frequency statistics corresponding to prior tasks. Let $\mathcal{C}^{1:t} = \bigcup_{i=1}^t \mathcal{C}^i$ represent the union of all classes seen up to task t . At the end of each epoch, we compute the overall class frequency $\mathbf{f} \in \mathbb{R}^{|\mathcal{C}^{1:t}|}$ by combining the pseudo-label distribution $\tilde{p}^t(c)$ derived from $\tilde{\mathbf{Y}}^t$ with the observed ground-truth label distribution $p^t(c)$ from the current task. The resulting frequency vector $\mathbf{f} = [f(c)]_{c \in \mathcal{C}^{1:t}}$ is then used to compute class-wise $\mathbf{w} = [w(c)]_{c \in \mathcal{C}^{1:t}}$ weights for balanced pseudo-label selection and to tune current model to favour rare classes.

During the next epoch, the model Φ^{t-1} produces soft pseudo-label predictions $\tilde{\mathbf{Y}}^t$, where each component $\tilde{\mathbf{Y}}^t[c]$ denotes the confidence score for class $c \in \mathcal{C}^{1:t-1}$. To promote balanced pseudo-label selection, we apply class-wise re-weighting using $w(c) = \frac{1}{f(c)+\epsilon}$, where ϵ is a small constant for numerical stability. The adjusted predictions are computed by applying the class-wise weights as: $\tilde{\mathbf{Y}}^{t,w}[c] = w(c) \cdot \tilde{\mathbf{Y}}^t[c]$, $\forall c \in \mathcal{C}^{1:t-1}$. We then perform top- K selection over both the original and the re-weighted scores, yielding two pseudo-label sets: $\tilde{\mathbf{Y}}_K^t$ and $\tilde{\mathbf{Y}}_K^{t,w}$, respectively. The final supervision label set $\bar{\mathbf{Y}}^t$ is constructed by concatenating the ground-truth labels \mathbf{Y}^t with both sets of pseudo-labels: $\bar{\mathbf{Y}}^t = \mathbf{Y}^t \parallel \tilde{\mathbf{Y}}_K^t \parallel \tilde{\mathbf{Y}}_K^{t,w}$.

Although the above re-weighting mitigates bias from prior tasks, it does not address class imbalance within the current task t . To resolve this, we extend the class-balanced weights w_c to incorporate statistics from both previously seen and current classes, i.e., over $\mathcal{C}^{1:t}$ rather than only $\mathcal{C}^{1:t-1}$, and denote the updated weights as w'_c , which are then integrated into the training objective. After incorporating all components, the modified objective in Eq. (1) becomes the final updated objective used in **CLIMB-3D**:

$$\mathcal{L}_{\text{CI-3DIS}}(\mathcal{D}_{\text{ER}}^t; \Phi^t) = \frac{1}{|\mathcal{D}_{\text{ER}}^t|} \sum_{(\mathbf{P}, \mathbf{Y}^t) \in \mathcal{D}_{\text{ER}}^t} \frac{1}{|\bar{\mathbf{Y}}^t|} \sum_{(\bar{m}_j^t, \bar{c}_j^t) \in \bar{\mathbf{Y}}^t} \left(\mathcal{L}_{\text{mask}}(\bar{m}_j^t, \hat{m}_j^t) + \mathbf{w}_c'' \cdot \mathcal{L}_{\text{cls}}(\bar{c}_j^t, \hat{c}_j^t) \right), \quad (5)$$

where $\mathbf{w}_c'' = \mathbf{w}'_c \cdot \lambda_{\text{cls}}$ denotes the scaled weight vector, and λ_{cls} is a loss-balancing hyperparameter. To address the class-imbalance across tasks, our CBR module jointly re-weights pseudo-label selection and classification loss, ensuring balanced supervision across all seen categories, including rare ones. This unified strategy reduces bias and enhances performance, particularly for under-represented classes.

3.3. Benchmarking Incremental Scenarios

While CI-3DIS methods offer a wide range of practical applications, they frequently rely on the assumption of uniform sample distribution – an assumption that rarely holds in real-world settings. In practice, the number of object categories, denoted by \mathcal{C} , is often large and characterised by

substantial variability in category frequency, shape, structure, and size. To address these challenges, we propose three incremental learning scenarios, each designed to capture a different facet of real-world complexity. The design of these scenarios is detailed below; for more information and illustration, please refer Appendix [Appendix C](#) of the supplementary material.

Split_A: Frequency Scenarios. This scenario acknowledges that datasets are often labelled based on the frequency of category occurrences. To accommodate this, we propose a split where the model initially learns from the most frequent categories and subsequently incorporates the less frequent ones in later stages. By prioritizing the training of frequently occurring categories, the model can establish a strong foundation before expanding its knowledge to handle rare categories.

Split_B: Semantic Scenarios. Beyond frequency, semantic similarity is crucial in real-world deployments. While objects often share visual or functional traits, models may encounter semantically different categories in new environment. To simulate this challenge, we introduce the **Split_B** scenario. Here, categories are grouped based on their semantic relationships, and the model is incrementally trained on one semantic group at a time. This setup encourages the model to generalise across semantically similar categories and adapt more effectively when exposed to new ones. Unlike the **Split_A** scenario, which organises learning based on category frequency, the **Split_B** scenario may contain both frequent and infrequent categories within a single task, focusing instead on semantic continuity and transfer.

Split_C: Random Scenarios. In some cases, data labelling is driven by the availability of objects rather than predefined criteria. To capture this, we introduce the **Split_C** scenario, which represents a fully random setting where any class can appear in any task, resulting in varying levels of class imbalance. By exposing the model to such diverse and unpredictable distributions, we aim to improve its robustness in real-world situations where labelled data availability is inconsistent.

By designing these incremental scenarios, we aim to provide a more realistic representation of object distributions, frequencies, and dynamics encountered in the real world.

4. Experiments

4.1. Setup

Datasets. We evaluate our method on the ScanNet200 [\[44\]](#), which comprises 200 object categories and exhibits significant class imbalance – making it ideal for simulating and assessing real-world scenarios. In addition, we benchmark our approach against existing incremental learning methods using the ScanNetV2 [\[13\]](#) in a 3DSS setting.

Table 1. Comparison between the proposed method and the baseline in the 3DIS setting, evaluated using mAP₂₅, mAP₅₀, mAP, and FPP after training across all phase.

Scenarios	Methods	Average Precision ↑			FPP ↓	
		mAP ₂₅	mAP ₅₀	mAP	mAP ₂₅	mAP ₅₀
Split_A	Baseline	16.46	14.29	10.44	51.30	46.82
	CLIMB-3D (Ours)	35.69	31.05	22.72	3.44	2.63
Split_B	Baseline	17.22	15.07	10.93	46.27	42.1
	CLIMB-3D (Ours)	35.48	31.56	23.69	8.00	5.51
Split_C	Baseline	25.65	21.08	14.85	31.68	28.84
	CLIMB-3D (Ours)	31.59	26.78	18.93	9.10	7.89

Table 2. Comparison between the proposed method and existing baselines in the 3DSS setting on ScanNetV2 [13], evaluated using mIoU.

Methods	Phase=1	Phase=2	All
EWC [47]	17.75	13.22	16.62
LwF [33]	30.38	13.37	26.13
Yang Yang et al. [57]	34.16	13.43	28.98
CLIMB-3D (Ours)	69.39	32.56	59.38

For this evaluation, we follow the standard training and validation splits defined in prior works [57].

Evaluation Metrics. We evaluate our method using *mean Average Precision* (mAP), a standard metric for 3DIS that provides a comprehensive measure of segmentation quality by accounting for both precision and recall. For comparison with existing 3DSS methods, we report the *mean Intersection over Union* (mIoU), which quantifies the overlap between predicted and ground truth segments. To assess the model’s ability to mitigate catastrophic forgetting in incremental settings, we use the *Forgetting Percentage Points* (FPP) metric, as defined in [37]. FPP captures performance degradation by measuring the accuracy drop on the initially seen categories between the first and final training phases.

Incremental Scenarios. As discussed in Section 3.3, we design three incremental scenarios – Split_A, Split_B, and Split_C – each with three tasks, based on object frequency, semantic similarity, and random grouping, respectively. For Split_A, we follow the class split provided by Rozenberszki et al. [44], with a class distribution of 66-68-66 across the three tasks. In Split_B, we partition the classes into 74-50-76 based on semantic similarity, which is calculated using the CLIP [40] text encoder, followed by clustering using K-Means. Finally, in Split_C, classes are randomly shuffled and split into three sets, with 67-67-66 categories per split. These scenarios comprehensively evaluate our approach’s performance and generalization in varied real-world condi-

tions.

Implementation Details. For all the experiments we use Mask3D [46] with the Minkowski Res16UNet34C [12] as a feature backbone. We adopt the data augmentation, hyperparameters, and training strategy described in [46], with using the AdamW optimizer [38] and a one-cycle learning rate scheduler [49], and results are evaluated on the entire validation set. In incremental training, learning is divided into three phases, introducing one split per phase across the three scenarios described in Sec. 3.3. For each phase, we train for 500, 300, and 300 epochs, respectively, except for the *Oracle* setting (Row 1 in Tab. 3), which is trained once for 600 epochs. We retain the same hyperparameters throughout, modifying only the number of training epochs. The exemplar replay size is fixed at $|\mathcal{E}^t| = 50$ scenes.

4.2. Results and Discussion

To evaluate our proposed approach, we construct a baseline using ER [3] for the 3DIS setting, as no existing incremental baselines are available for this task. In contrast, for the 3DSS setting, where prior incremental baselines do exist, we compare our method against three existing approaches [33, 47, 57].

Results on CI-3DIS. Tab. 1 compares **CLIMB-3D** against the ER baseline across three CI-3DIS scenarios, evaluated after all phases using mAP₂₅, mAP₅₀, overall mAP, and FPP. In the Split_A scenario, characterized by significant distribution shifts, it achieves gains of +19.23%, +16.76%, and +12.28% in mAP₂₅, mAP₅₀, and overall mAP, while drastically reducing forgetting with FPP scores of 3.44% and 2.63%, over 47 points lower than the baseline. Under the Split_B scenario, with semantically related new categories, improvements of +18.26%, +16.49%, and +12.76% are observed alongside a reduction in forgetting to 8.00% and 5.51% from baseline levels above 42%. For the Split_C scenario, featuring increasing geometric complexity, it maintains solid gains of +5.94%, +5.70%, and +4.08% across mAP metrics, with forgetting reduced by over 22 points. Overall, these results demonstrate robust

Table 3. Ablation study showing the impact of each component ER, PLG, and CBR in a three-phase setup. Each split (**s**) and number corresponds to data introduced at that phase. The **All** column reports performance over all classes seen so far. Joint training (Oracle) is highlighted in gray, and the full model in orange. Best results are in **bold**.

Row	Modules	p=1 ↑			p=2 ↑			p=3 ↑				FPP ↓
		s1	s1	s2	All	s1	s2	s3	All			
1.	Oracle	-	-	-	-	55.14	30.77	25.30	37.68	-		
2.	Naïve	56.82	0.00	28.09	14.15	0.00	0.00	19.67	5.80	56.82		
3.	+ ER	56.82	18.51	32.81	25.72	10.38	9.43	24.27	14.28	46.44		
4.	+ PLG	56.82	50.00	34.39	42.13	49.78	11.41	26.47	29.28	7.04		
5.	+ CBR	56.82	54.67	33.75	44.13	54.19	12.02	26.55	31.05	2.63		

forward transfer, minimal forgetting, and stable learning, validating the method’s effectiveness for scalable continual 3D semantic understanding.

Results on CI-3DSS. Although our primary focus is on CI-3DIS, we additionally evaluate our method under the CI-3DSS setting to enable comparison with existing approaches. For this, we adapt our predictions by assigning each point the label corresponding to the highest-confidence mask and exclude background classes (floor and wall), as these are not part of the semantic segmentation targets. Tab. 2 presents a comparison between our method and existing baselines on the ScanNet V2 dataset [13], evaluated using mIoU across two training phases and overall. Despite being designed for instance segmentation, our method generalises effectively to semantic segmentation, achieving substantial gains: +35.23% mIoU in Phase 1 and +19.1% in Phase 2. Overall, it achieves 59.38% mIoU – significantly higher than the ∼30% mIoU of prior methods – highlighting its robustness and transferability.

For a detailed per-phase analysis, evaluation of rare classes, and qualitative result comparisons, please refer to Appendix Appendix A, Appendix Appendix B, and Appendix Appendix D, respectively, in the supplementary material.

4.3. Ablation

We conduct an ablation study to evaluate the contribution of each component in our framework. As an upper bound, we report the performance of an *Oracle* model trained jointly on the full dataset. For the incremental setting, we follow the previously defined splits and first train the model naively across phases. We then incrementally add each module to isolate its impact. Tab. 3 presents results on the Split_Ascenario using both mAP₅₀ and FPP metrics.

Naïve Training. When trained naïvely without any dedicated modules, the model suffers from severe catastrophic forgetting, as evident in row 2. The model completely forgets previously learned classes upon entering new phases, with performance dropping to zero for earlier splits and a

high FPP of 56.82.

Effect of ER. Adding exemplar replay (row 3) partially alleviates forgetting by maintaining a buffer of past examples. This yields notable gains for **s1** in phase 2 (+18.51%) and phase 3 (+10.38%), and also improves **s2** in phase 3 (+9.43%). However, the overall forgetting remains substantial (FPP: 46.44), showing ER alone is insufficient.

Effect of PLG. The addition of the pseudo-label generator (PLG), which generates labels for previous classes by retaining a copy of the model from earlier phase, facilitates knowledge retention and forward transfer. As shown in row 4, PLG significantly reduces forgetting and enhances performance on current tasks. For **s1**, it improves mAP₅₀ by 31.49% in phase 2 and 39.40% in phase 3 over exemplar replay. Overall, PLG yields a 15.00% increase in performance and reduces forgetting by 39.40%.

Effect of CBR. Finally, class-balanced re-weighting (CBR) mitigates class imbalance both during pseudo-labelling and current task learning by adjusting each class’s contribution based on its frequency. As shown in row 5, CBR enhances **s1** retention over PLG in phases 2 and 3 (+4.67% and +4.41%) and further improves performance on **s2** and **s3**. It also achieves the lowest FPP of 2.63, reflecting effective forgetting mitigation. Overall, CBR offers the best trade-off between retaining past knowledge and learning new tasks, outperforming PLG and ER by 4.41% and 43.81%, respectively.

5. Conclusion

We address the critical challenge of catastrophic forgetting in class-incremental 3D instance segmentation by proposing a modular framework that combines exemplar replay (ER), a pseudo-label generator (PLG), and class-balanced re-weighting (CBR). Our method incrementally adapts to new classes while preserving knowledge from previous tasks without requiring access to the full dataset. Through extensive experiments on a three-phase benchmark, we demonstrate the individual and combined effectiveness of each component. ER provides a easy knowledge storage,

PLG enhances knowledge retention via pseudo-label supervision, and CBR further refines learning by mitigating class imbalance. Together, these modules significantly reduce forgetting and improve overall segmentation performance across all phases. By balancing stability and plasticity, our method contributes to continual 3D scene understanding and establishing a new baseline for future research.

References

Tel Aviv, Israel, October 23–27, 2022, Proceedings, Part XXXI, pages 681–699. Springer, 2022. [2](#)

[1] Rahaf Aljundi, Francesca Babiloni, Mohamed Elhoseiny, Marcus Rohrbach, and Tinne Tuytelaars. Memory aware synapses: Learning what (not) to forget. In *In Proceedings of the European Conference on Computer Vision*, pages 139–154, 2018. [1](#), [2](#), [3](#)

[2] Mohamed El Amine Boudjoghra, Salwa Al Khatib, Jean La-houd, Hisham Cholakkal, Rao Anwer, Salman H Khan, and Fahad Shahbaz Khan. 3d indoor instance segmentation in an open-world. *Advances in Neural Information Processing Systems*, 36, 2024. [1](#), [3](#), [4](#)

[3] Pietro Buzzega, Matteo Boschini, Angelo Porrello, Davide Abati, and Simone Calderara. Dark experience for general continual learning: a strong, simple baseline. *Advances in Neural Information Processing Systems*, 33:15920–15930, 2020. [3](#), [6](#)

[4] Fabio Cermelli, Massimiliano Mancini, Samuel Rota Bulo, Elisa Ricci, and Barbara Caputo. Modeling the background for incremental learning in semantic segmentation. In *Proceedings of the IEEE/CVF Conference on Computer Vision and Pattern Recognition*, pages 9233–9242, 2020. [1](#)

[5] Fabio Cermelli, Dario Fontanel, Antonio Tavera, Marco Ciccone, and Barbara Caputo. Incremental learning in semantic segmentation from image labels. In *Proceedings of the IEEE/CVF Conference on Computer Vision and Pattern Recognition*, pages 4371–4381, 2022. [1](#)

[6] Hyuntak Cha, Jaeho Lee, and Jinwoo Shin. Co2l: Contrastive continual learning. In *Proceedings of the IEEE/CVF International Conference on Computer Vision*, pages 9516–9525, 2021. [3](#)

[7] Shaoyu Chen, Jiemin Fang, Qian Zhang, Wenyu Liu, and Xinggang Wang. Hierarchical aggregation for 3d instance segmentation. In *Proceedings of the IEEE/CVF International Conference on Computer Vision*, pages 15467–15476, 2021. [2](#)

[8] Bowen Cheng, Alex Schwing, and Alexander Kirillov. Per-pixel classification is not all you need for semantic segmentation. *Advances in Neural Information Processing Systems*, 34:17864–17875, 2021. [2](#)

[9] Bowen Cheng, Ishan Misra, Alexander G Schwing, Alexander Kirillov, and Rohit Girdhar. Masked-attention mask transformer for universal image segmentation. In *Proceedings of the IEEE/CVF Conference on Computer Vision and Pattern Recognition*, pages 1290–1299, 2022. [2](#)

[10] Julian Chibane, Francis Engelmann, Tuan Anh Tran, and Gerard Pons-Moll. Box2mask: Weakly supervised 3d semantic instance segmentation using bounding boxes. In *Computer Vision–ECCV 2022: 17th European Conference*, Tel Aviv, Israel, October 23–27, 2022, Proceedings, Part XXXI, pages 681–699. Springer, 2022. [2](#)

[11] Townim Chowdhury, Mahira Jalisha, Ali Cheraghian, and Shafin Rahman. Learning without forgetting for 3d point cloud objects. In *Advances in Computational Intelligence: 16th International Work-Conference on Artificial Neural Networks, IWANN 2021, Virtual Event, June 16–18, 2021, Proceedings, Part I 16*, pages 484–497. Springer, 2021. [1](#)

[12] Christopher Choy, JunYoung Gwak, and Silvio Savarese. 4d spatio-temporal convnets: Minkowski convolutional neural networks. In *Proceedings of the IEEE/CVF conference on computer vision and pattern recognition*, pages 3075–3084, 2019. [6](#)

[13] Angela Dai, Angel X. Chang, Manolis Savva, Maciej Halber, Thomas Funkhouser, and Matthias Nießner. Scannet: Richly-annotated 3d reconstructions of indoor scenes. In *Proc. Computer Vision and Pattern Recognition (CVPR), IEEE*, 2017. [5](#), [6](#), [7](#)

[14] Matthias De Lange, Rahaf Aljundi, Marc Masana, Sarah Parisot, Xu Jia, Aleš Leonardis, Gregory Slabaugh, and Tinne Tuytelaars. A continual learning survey: Defying forgetting in classification tasks. *IEEE transactions on pattern analysis and machine intelligence*, 44(7):3366–3385, 2021. [1](#)

[15] Jiahua Dong, Yang Cong, Gan Sun, Bingtao Ma, and Lichen Wang. I3dol: Incremental 3d object learning without catastrophic forgetting. In *Proceedings of the AAAI Conference on Artificial Intelligence*, pages 6066–6074, 2021. [1](#)

[16] Arthur Douillard, Yifu Chen, Arnaud Dapogny, and Matthieu Cord. Plop: Learning without forgetting for continual semantic segmentation. In *Proceedings of the IEEE/CVF conference on computer vision and pattern recognition*, pages 4040–4050, 2021. [1](#)

[17] Francis Engelmann, Martin Bokeloh, Alireza Fathi, Bastian Leibe, and Matthias Nießner. 3d-mpa: Multi-proposal aggregation for 3d semantic instance segmentation. In *Proceedings of the IEEE/CVF conference on computer vision and pattern recognition*, pages 9031–9040, 2020. [2](#)

[18] Lei Han, Tian Zheng, Lan Xu, and Lu Fang. Occuseg: Occupancy-aware 3d instance segmentation. In *Proceedings of the IEEE/CVF conference on computer vision and pattern recognition*, pages 2940–2949, 2020. [2](#)

[19] Tong He, Chunhua Shen, and Anton Van Den Hengel. Dyco3d: Robust instance segmentation of 3d point clouds through dynamic convolution. In *Proceedings of the IEEE/CVF conference on computer vision and pattern recognition*, pages 354–363, 2021. [2](#)

[20] Geoffrey Hinton, Oriol Vinyals, Jeff Dean, et al. Distilling the knowledge in a neural network. *arXiv preprint arXiv:1503.02531*, 2(7), 2015. [2](#)

[21] Ji Hou, Angela Dai, and Matthias Nießner. 3d-sis: 3d semantic instance segmentation of rgbd scans. In *Proceedings of the IEEE/CVF conference on computer vision and pattern recognition*, pages 4421–4430, 2019. [1](#), [2](#)

[22] Ji Hou, Benjamin Graham, Matthias Nießner, and Saining Xie. Exploring data-efficient 3d scene understanding with contrastive scene contexts. In *Proceedings of the IEEE/CVF*

Conference on Computer Vision and Pattern Recognition, pages 15587–15597, 2021. 2

[23] Chao Jia, Yinfai Yang, Ye Xia, Yi-Ting Chen, Zarana Parekh, Hieu Pham, Quoc Le, Yun-Hsuan Sung, Zhen Li, and Tom Duerig. Scaling up visual and vision-language representation learning with noisy text supervision. In *International Conference on Machine Learning*, pages 4904–4916. PMLR, 2021. 1

[24] Li Jiang, Hengshuang Zhao, Shaoshuai Shi, Shu Liu, Chi-Wing Fu, and Jiaya Jia. Pointgroup: Dual-set point grouping for 3d instance segmentation. In *Proceedings of the IEEE/CVF conference on computer vision and Pattern recognition*, pages 4867–4876, 2020. 2

[25] KJ Joseph, Salman Khan, Fahad Shahbaz Khan, and Vineeth N Balasubramanian. Towards open world object detection. In *Proceedings of the IEEE/CVF conference on computer vision and pattern recognition*, pages 5830–5840, 2021. 1

[26] Nitin Kamra, Umang Gupta, and Yan Liu. Deep generative dual memory network for continual learning. *arXiv preprint arXiv:1710.10368*, 2017. 3

[27] Zixuan Ke, Bing Liu, and Xingchang Huang. Continual learning of a mixed sequence of similar and dissimilar tasks. *Advances in Neural Information Processing Systems*, 33: 18493–18504, 2020. 3

[28] James Kirkpatrick, Razvan Pascanu, Neil Rabinowitz, Joel Veness, Guillaume Desjardins, Andrei A Rusu, Kieran Milan, John Quan, Tiago Ramalho, Agnieszka Grabska-Barwinska, et al. Overcoming catastrophic forgetting in neural networks. *Proceedings of the national academy of sciences*, 114(13):3521–3526, 2017. 2

[29] Theodora Kontogianni, Yuanwen Yue, Siyu Tang, and Konrad Schindler. Is continual learning ready for real-world challenges? *arXiv preprint arXiv:2402.10130*, 2024. 3

[30] Jean Lahoud, Bernard Ghanem, Marc Pollefeys, and Martin R Oswald. 3d instance segmentation via multi-task metric learning. In *Proceedings of the IEEE/CVF International Conference on Computer Vision*, pages 9256–9266, 2019. 2

[31] Xin Lai, Jianhui Liu, Li Jiang, Liwei Wang, Hengshuang Zhao, Shu Liu, Xiaojuan Qi, and Jiaya Jia. Stratified transformer for 3d point cloud segmentation, 2022. 1

[32] Xilai Li, Yingbo Zhou, Tianfu Wu, Richard Socher, and Caiming Xiong. Learn to grow: A continual structure learning framework for overcoming catastrophic forgetting. In *International Conference on Machine Learning*, pages 3925–3934. PMLR, 2019. 3

[33] Zhizhong Li and Derek Hoiem. Learning without forgetting. *IEEE transactions on pattern analysis and machine intelligence*, 40(12):2935–2947, 2017. 1, 2, 3, 6

[34] Zhihao Liang, Zhihao Li, Songcen Xu, Mingkui Tan, and Kui Jia. Instance segmentation in 3d scenes using semantic superpoint tree networks. In *Proceedings of the IEEE/CVF International Conference on Computer Vision*, pages 2783–2792, 2021. 2

[35] Shih-Hung Liu, Shang-Yi Yu, Shao-Chi Wu, Hwann-Tzong Chen, and Tyng-Luh Liu. Learning gaussian instance segmentation in point clouds. *arXiv preprint arXiv:2007.09860*, 2020. 2

[36] Yuyang Liu, Yang Cong, Gan Sun, Tao Zhang, Jiahua Dong, and Hongsen Liu. L3doc: Lifelong 3d object classification. *IEEE Transactions on Image Processing*, 30:7486–7498, 2021. 1

[37] Yaoyao Liu, Bernt Schiele, Andrea Vedaldi, and Christian Rupprecht. Continual detection transformer for incremental object detection. In *Proceedings of the IEEE/CVF Conference on Computer Vision and Pattern Recognition*, pages 23799–23808, 2023. 1, 6

[38] Ilya Loshchilov and Frank Hutter. Decoupled weight decay regularization. *arXiv preprint arXiv:1711.05101*, 2017. 6

[39] Michael McCloskey and Neal J Cohen. Catastrophic interference in connectionist networks: The sequential learning problem. In *Psychology of learning and motivation*, pages 109–165. Elsevier, 1989. 1, 3

[40] Alec Radford, Jong Wook Kim, Chris Hallacy, Aditya Ramesh, Gabriel Goh, Sandhini Agarwal, Girish Sastry, Amanda Askell, Pamela Mishkin, Jack Clark, et al. Learning transferable visual models from natural language supervision. In *International Conference on Machine Learning*, pages 8748–8763. PMLR, 2021. 6

[41] Jathushan Rajasegaran, Munawar Hayat, Salman Khan, Fahad Shahbaz Khan, and Ling Shao. Random path selection for incremental learning. *Advances in Neural Information Processing Systems*, 3, 2019. 3

[42] Sylvestre-Alvise Rebuffi, Alexander Kolesnikov, Georg Sperl, and Christoph H Lampert. icarl: Incremental classifier and representation learning. In *Proceedings of the IEEE/CVF Conference on Computer Vision and Pattern Recognition*, pages 2001–2010, 2017. 1, 3

[43] David Rolnick, Arun Ahuja, Jonathan Schwarz, Timothy Lillicrap, and Gregory Wayne. Experience replay for continual learning. *Advances in Neural Information Processing Systems*, 32, 2019. 1

[44] David Rozenberszki, Or Litany, and Angela Dai. Language-grounded indoor 3d semantic segmentation in the wild. In *Proceedings of the European Conference on Computer Vision (ECCV)*, 2022. 2, 5, 6, 11

[45] Andrei A Rusu, Neil C Rabinowitz, Guillaume Desjardins, Hubert Soyer, James Kirkpatrick, Koray Kavukcuoglu, Razvan Pascanu, and Raia Hadsell. Progressive neural networks. *arXiv preprint arXiv:1606.04671*, 2016. 3

[46] Jonas Schult, Francis Engelmann, Alexander Hermans, Or Litany, Siyu Tang, and Bastian Leibe. Mask3D: Mask Transformer for 3D Semantic Instance Segmentation. In *International Conference on Robotics and Automation (ICRA)*, 2023. 1, 2, 6

[47] Joan Serra, Didac Suris, Marius Miron, and Alexandros Karatzoglou. Overcoming catastrophic forgetting with hard attention to the task. In *International Conference on Machine Learning*, pages 4548–4557. PMLR, 2018. 1, 2, 6

[48] Konstantin Shmelkov, Cordelia Schmid, and Karteek Alahari. Incremental learning of object detectors without catastrophic forgetting. In *Proceedings of the IEEE international conference on computer vision*, pages 3400–3409, 2017. 1

[49] Leslie N Smith and Nicholay Topin. Super-convergence: Very fast training of neural networks using large learning rates. In *Artificial intelligence and machine learning*

for multi-domain operations applications, pages 369–386. SPIE, 2019. 6

[50] Yuanzhi Su, Siyuan Chen, and Yuan-Gen Wang. Balanced residual distillation learning for 3d point cloud class-incremental semantic segmentation. *arXiv preprint arXiv:2408.01356*, 2024. 3

[51] Jiahao Sun, Chunmei Qing, Junpeng Tan, and Xiangmin Xu. Superpoint transformer for 3d scene instance segmentation. *arXiv preprint arXiv:2211.15766*, 2022. 2

[52] Ashish Vaswani, Noam Shazeer, Niki Parmar, Jakob Uszkoreit, Llion Jones, Aidan N Gomez, Łukasz Kaiser, and Illia Polosukhin. Attention is all you need. *Advances in Neural Information Processing Systems*, 30, 2017. 2

[53] Weiyue Wang, Ronald Yu, Qiangui Huang, and Ulrich Neumann. Sgpn: Similarity group proposal network for 3d point cloud instance segmentation. In *Proceedings of the IEEE conference on computer vision and pattern recognition*, pages 2569–2578, 2018. 1, 2

[54] Zifeng Wang, Tong Jian, Kaushik Chowdhury, Yanzhi Wang, Jennifer Dy, and Stratis Ioannidis. Learn-prune-share for lifelong learning. In *2020 IEEE International Conference on Data Mining (ICDM)*, pages 641–650. IEEE, 2020. 3

[55] Saining Xie, Jiatao Gu, Demi Guo, Charles R Qi, Leonidas Guibas, and Or Litany. Pointcontrast: Unsupervised pre-training for 3d point cloud understanding. In *Computer Vision–ECCV 2020: 16th European Conference, Glasgow, UK, August 23–28, 2020, Proceedings, Part III 16*, pages 574–591. Springer, 2020. 2

[56] Bo Yang, Jianan Wang, Ronald Clark, Qingyong Hu, Sen Wang, Andrew Markham, and Niki Trigoni. Learning object bounding boxes for 3d instance segmentation on point clouds. *Advances in neural information processing systems*, 32, 2019. 1, 2

[57] Yuwei Yang, Munawar Hayat, Zhao Jin, Chao Ren, and Yinjie Lei. Geometry and uncertainty-aware 3d point cloud class-incremental semantic segmentation. In *Proceedings of the IEEE/CVF Conference on Computer Vision and Pattern Recognition (CVPR)*, pages 21759–21768, 2023. 1, 3, 6

[58] Li Yi, Wang Zhao, He Wang, Minhyuk Sung, and Leonidas J Guibas. Gspn: Generative shape proposal network for 3d instance segmentation in point cloud. In *Proceedings of the IEEE/CVF Conference on Computer Vision and Pattern Recognition*, pages 3947–3956, 2019. 2

[59] Biao Zhang and Peter Wonka. Point cloud instance segmentation using probabilistic embeddings. In *Proceedings of the IEEE/CVF Conference on Computer Vision and Pattern Recognition*, pages 8883–8892, 2021. 1, 2

[60] Tingting Zhao, Zifeng Wang, Aria Masoomi, and Jennifer Dy. Deep bayesian unsupervised lifelong learning. *Neural Networks*, 149:95–106, 2022. 3

CLIMB-3D: Continual Learning for Imbalanced 3D Instance Segmentation

Supplementary Material

In this supplementary material, we first present the per-phase performance of the proposed **CLIMB-3D** model in Appendix [Appendix A](#), followed by the analysis of gains on rare classes achieved through the incorporation of the CBR module in Appendix [Appendix B](#). Next, we provide detailed split information for all scenarios, based on class names, in Appendix [Appendix C](#). Finally, we present a qualitative comparison between the baseline method and our proposed approach in Appendix [Appendix D](#).

Appendix A. Per-Phase Performance Analysis

We extend the analysis presented in Tab. 1 (Sec. 4.2 of the main paper) to Tab. 4 to examine the impact of our proposed method across individual splits and phases in different scenarios. The results consistently show that our method outperforms the baseline by better retaining knowledge from earlier tasks.

Split_A. In the Split_A scenario, our model shows notable improvements across all phases. Particularly in Phase 3, although both methods show a drop in performance for s2, our approach significantly reduces forgetting, maintaining a higher mAP₅₀ across all splits.

Split_B. The Split_B scenario, while more challenging due to increased semantic overlap, demonstrates our model’s strength in generalisation. In Phase 2, it achieves an overall mAP₅₀ of 43.13% compared to the baseline’s 24.53%. This trend continues in Phase 3, with our model achieving 31.56%, more than double the baseline’s 15.07%, indicating both improved learning and retention.

Split_C. For the Split_C scenario, where splits are randomly grouped, Phase 1 performance is initially lower. However, in subsequent phases, our method balances stability and plasticity better than the baseline. By Phase 3, it consolidates performance across all splits, improving the overall mAP₅₀ to 26.78%, a 5.7% gain over the baseline.

These results demonstrate the robustness of our method in handling continual learning under varied and challenging split strategies.

Appendix B. Evaluation on Rare Categories

The proposed Class-Balanced Re-weighting (CBR) module, as detailed in [3.2](#), is designed to address the performance gap for rare classes. To assess its impact, we compare its performance with the framework which has exemplar replay (ER) and Pseudo-Label Generator (PLG). Specifically, we focus on its ability to improve performance

for rare classes, which the model encounters infrequently compared to more common classes.

The results, shown in Tab. 5 and Table 6, correspond to evaluations on Split_A for *Phase 2* and *Phase 3*, respectively. In *Phase 2*, we evaluate classes seen 1–20 times per epoch, while *Phase 3* targets even less frequent classes, with observations limited to 1–10 times per epoch.

As illustrated in Table 5, the CBR module substantially improves performance on rare classes in terms of mAP₅₀ in Phase 2 of Split_A. For instance, classes like recycling bin and trash bin, seen only 3 and 7 times, respectively, show significant improvement when the CBR module is applied. Overall, the CBR module provides an average boost of 8.32%, highlighting its effectiveness in mitigating class imbalance.

Similarly, Table 6 presents results for *Phase 3*, demonstrating significant gains for infrequent classes. For example, even though classes such as piano, bucket, and laundry basket are observed only once, the CBR module improves the performance by 52.30%, 10.40%, and 13.60%, respectively. The ER+PLG module does not focus on rare classes like shower and toaster, which results in low performance, but the CBR module compensates for this imbalance by focusing on underrepresented categories. On average, the addition of the proposed CBR module into the framework outperforms ER+PLG by 12.13%.

Appendix C. Incremental Scenarios Phases

Table 7 presents the task splits for each proposed scenario introduced in Sec. 3.3, and Fig. 3 illustrates them visually for the ScanNet200 [\[44\]](#) dataset. The three scenarios – Split_A, Split_B, and Split_C – are each divided into three tasks: Task1, Task2, and Task3. Notably, the order of classes within these tasks is random.

Appendix D. Qualitative Results

In this section, we present a qualitative comparison of the proposed framework with the baseline method. Figure 4 illustrates the results on the Split_A evaluation after learning all tasks, comparing the performance of the baseline method and our proposed approach. As shown in the figure, our method demonstrates superior instance segmentation performance compared to the baseline. For example, in row 1, the baseline method fails to segment the sink, while in row 3, the sofa instance is missed. Overall, our framework consistently outperforms the baseline, with several missed instances by the baseline highlighted in red circles.

Table 4. Comparison of results in terms of mAP₅₀ with and proposed CLIMB-3D for three different scenarios. Each scenario is trained in three phases (phase = 1, 2, 3) by introducing a single split s at a time. The results highlighted in orange are with the proposed method, and the best results for each scenario are in **bold**.

Scenarios	Methods	phase=1			phase=2			phase=3			
		s1	s1	s2	All	s1	s2	s3	All		
Split_A	Baseline	56.82	18.51	32.81	25.72	10.38	9.43	24.27	14.28		
	CLIMB-3D	56.82	54.67	33.75	44.13	54.19	12.02	26.55	31.05		
Split_B	Baseline	51.57	13.32	42.21	24.53	9.55	12.45	26.78	15.07		
	CLIMB-3D	51.57	46.74	37.45	43.13	46.06	15.95	26.68	31.56		
Split_C	Baseline	36.40	7.74	37.62	22.32	7.55	15.96	40.41	21.08		
	CLIMB-3D	36.40	32.63	33.38	33.00	28.51	17.11	34.64	26.78		

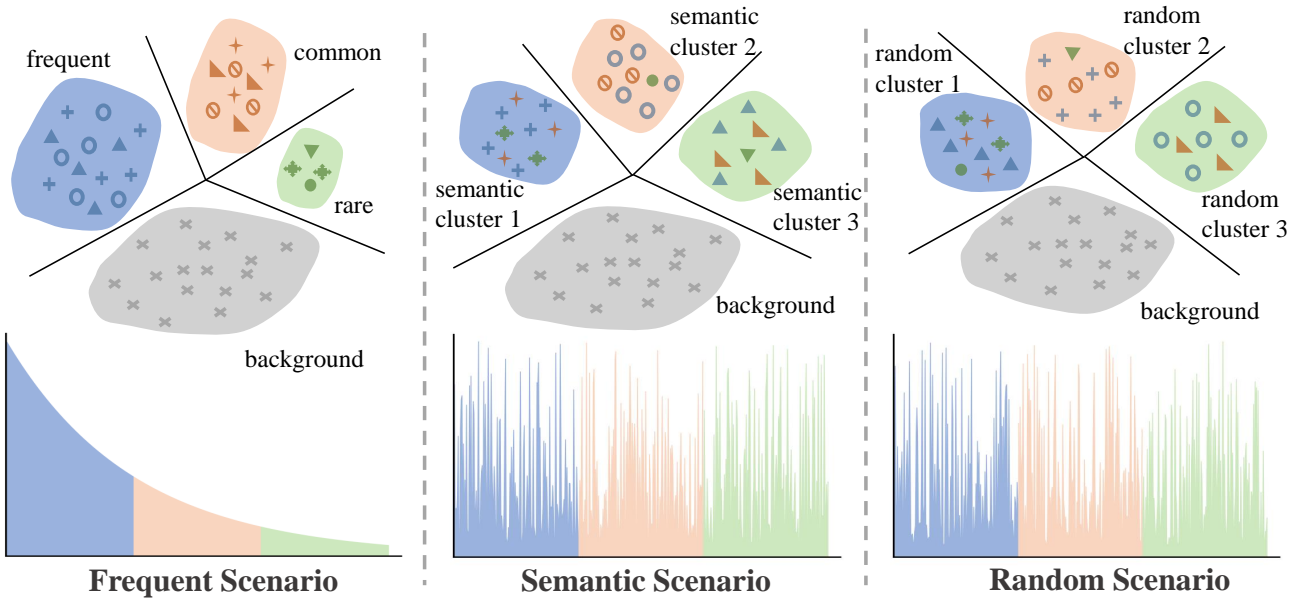


Figure 3. Tasks are grouped into incremental scenarios based on object frequency, semantic similarity, and random assignment. ■, □, and ▲ denote different tasks; shapes indicate object categories; □ marks the background. **Left:** Grouped by category frequency. **Middle:** Grouped by semantic similarity (e.g., similar shapes). **Right:** Randomly grouped, mixing semantic and frequency variations.

In Figure 5, we present the results on Split_B, highlighting instances where the baseline method underperforms, marked with red circles. For example, in row 2, the baseline method incorrectly identifies the same sofa as separate instances. Similarly, in row 5, the washing machine is segmented into two instances by the baseline. In contrast, the proposed method delivers results that closely align with the ground truth, demonstrating its superior performance.

Similarly, Figure 6 highlights the results on Split_C, where classes are encountered in random order. The comparison emphasizes the advantages of our method, as highlighted by red circles. The baseline method often misses instances or splits a single instance into multiple parts. In contrast, our approach consistently produces results that are closely aligned with the ground truth, further underscoring

its effectiveness.

Table 5. Results for classes observed by the model 1–20 times during an epoch, evaluated on Split_A for Phase 2, in terms of mAP₅₀.

Classes	Seen Count	ER+KD	ER+KD+IC
paper towel dispenser	2	73.10	74.90
recycling bin	3	55.80	60.50
ladder	5	53.90	57.10
trash bin	7	31.50	57.30
bulletin board	8	23.30	38.20
shelf	11	48.00	50.50
dresser	12	44.00	55.80
copier	12	93.30	94.50
object	12	3.10	3.30
stairs	13	51.70	67.70
bathtub	16	80.30	86.60
oven	16	1.50	3.30
divider	18	36.40	45.00
column	20	57.30	75.00
Average	-	46.66	54.98

Table 6. Results for classes observed by the model 1–10 times during an epoch, evaluated on Split_A for Phase 3, in terms of mAP₅₀.

Classes	Seen Count	ER+KD	ER+KD+IC
piano	1	7.10	59.40
bucket	1	21.10	31.50
laundry basket	1	3.80	17.40
dresser	2	55.00	55.40
paper towel dispenser	2	32.50	35.50
cup	2	24.70	30.30
bar	2	35.40	39.50
divider	2	28.60	42.40
case of water bottles	2	0.00	1.70
shower	3	0.00	45.50
mirror	8	56.00	68.80
trash bin	4	1.10	2.70
backpack	5	74.50	76.70
copier	5	94.00	96.80
bathroom counter	3	3.90	20.30
ottoman	4	32.60	36.20
storage bin	3	5.10	10.50
dishwasher	3	47.40	66.20
trash bin	4	1.10	2.70
backpack	5	74.50	76.70
copier	5	94.00	96.80
sofa chair	6	14.10	43.50
file cabinet	6	49.20	57.60
tv stand	7	67.70	68.60
mirror	8	56.00	68.80
blackboard	8	57.10	82.80
clothes dryer	9	1.70	3.20
toaster	9	0.10	25.90
wardrobe	10	22.80	58.80
jacket	10	1.20	4.10
Average	-	32.08	44.21

Table 7. Classes grouped by tasks for each proposed scenario on the ScanNet200 dataset labels. The three scenarios Split_A, Split_B, and Split_C are each divided into three tasks: Task 1, Task 2, and Task 3.

Split_A			Split_B			Split_C		
Task 1	Task 2	Task 3	Task 1	Task 2	Task 3	Task 1	Task 2	Task 3
chair	wall	pillow	tv stand	cushion	paper	broom	fan	rack
table	floor	picture	curtain	end table	plate	towel	stove	music stand
couch	door	book	blinds	dining table	soap dispenser	fireplace	tv	bed
desk	cabinet	box	shower curtain	keyboard	bucket	blanket	dustpan	soap dish
office chair	shelf	lamp	bookshelf	bag	clock	dining table	sink	closet door
bed	window	towel	tv	toilet paper	guitar	shelf	toaster	basket
sink	bookshelf	clothes	kitchen cabinet	printer	toilet paper holder	rail	doorframe	chair
toilet	curtain	cushion	pillow	blanket	speaker	bathroom counter	wall	toilet paper
monitor	Kitchen cabinet	plant	lamp	microwave	cup	plunger	mattress	ball
armchair	counter	bag	dresser	shoe	paper towel roll	bin	stand	monitor
coffee table	ceiling	backpack	monitor	computer tower	bar	armchair	copier	bathroom cabinet
refrigerator	whiteboard	toilet paper	object	bottle	toaster	trash bin	ironing board	shoe
tv	shower curtain	blanket	ceiling	bin	ironing board	dishwasher	radiator	blackboard
nightstand	closet	shoe	board	ottoman	soap dish	lamp	keyboard	vent
dresser	computer tower	bottle	stove	bench	toilet paper dispenser	projector	toaster oven	bag
stool	board	basket	closet wall	basket	fire extinguisher	potted plant	paper bag	paper
bathtub	mirror	fan	couch	fan	ball	coat rack	structure	projector screen
end table	shower	paper	office chair	laptop	hat	end table	picture	pillar
dining table	blinds	person	kitchen counter	person	shower curtain rod	tissue box	purse	range hood
keyboard	rack	plate	shower	paper towel dispenser	paper cutter	stairs	tray	coffee maker
printer	blackboard	container	closet	oven	tray	fire extinguisher	couch	handicap bar
tv stand	rail	soap dispenser	doorframe	rack	toaster oven	case of water bottles	telephone	pillow
trash can	radiator	telephone	sofa chair	piano	mouse	water bottle	shower curtain rod	decoration
stairs	wardrobe	bucket	mailbox	suitcase	toilet seat cover dispenser	ledge	trash can	printer
microwave	column	clock	nightstand	rail	storage container	shower head	closet wall	object
stove	ladder	stand	washing machine	container	scale	guitar case	cart	mirror
bin	bathroom stall	light	picture	telephone	tissue box	kitchen cabinet	hat	ottoman
ottoman	shower wall	pipe	book	stand	light switch	poster	paper cutter	water pitcher
bench	mat	guitar	sink	light	crate	candle	storage organizer	refrigerator
washing machine	window sill	toilet paper holder	recycling bin	laundry basket	power outlet	bowl	vacuum cleaner	divider
copier	bulletin board	speaker	table	pipe	sign	plate	mouse	toilet
sofa chair	doorframe	bicycle	backpack	seat	projector	person	paper towel roll	washing machine
file cabinet	shower curtain rod	cup	shower wall	column	candle	storage bin	laundry detergent	mat
laptop	paper cutter	jacket	toilet	bicycle	plunger	microwave	calendar	scale
paper towel dispenser	shower door	paper towel roll	copier	ladder	stuffed animal	office chair	wardrobe	dresser
oven	pillar	machine	counter	jacket	headphones	clothes dryer	whiteboard	bookshelf
piano	ledge	soap dish	stool	storage bin	broom	headphones	laundry basket	tv stand
suitcase	light switch	fire extinguisher	refrigerator	coffee maker	guitar case	toilet seat cover dispenser	shower door	closet rod
recycling bin	closet door	ball	window	dishwasher	storage bin	bathroom stall door	curtain	plant
laundry basket	shower floor	hat	file cabinet	machine	microwave	speaker	folded chair	counter
clothes dryer	projector screen	water cooler	chair	mat	office chair	keyboard piano	suitcase	bench
seat	divider	mouse	wall	window sill	headphones	clothes dryer	hair dryer	ceiling
storage bin	closet wall	scale	plant	bulletin board	storage bin	headphones	mini fridge	piano
coffee maker	bathroom stall door	power outlet	coffee table	fireplace	purse	toilet seat cover dispenser	shower door	closet
dishwasher	stair rail	decoration	stairs	mini fridge	vent	bathroom stall door	curtain	cabinet
bar	bathroom cabinet	sign	armchair	water cooler	shower floor	speaker	folded chair	counter
toaster	closet rod	projector	cabinet	water pitcher	water pitcher	keyboard piano	suitcase	bench
ironing board	structure	vacuum cleaner	bathroom vanity	pillar	bowl	clothes dryer	hair dryer	ceiling
fireplace	coat rack	candle	bathroom stall	ledge	alarm clock	headphones	mini fridge	piano
kitchen counter	plunger	stuffed animal	mirror	furniture	music stand	toilet seat cover dispenser	shower door	closet
toilet paper dispenser	headphones	trash can	blackboard	cart	laundry detergent	storage bin	curtain	plant
mini fridge	broom	stair rail	closet door	pillar	dumbbell	toilet paper dispenser	shower door	counter
tray	guitar case	box	vacuum cleaner	ledge	paper bag	coffee table	curtain	bench
toaster oven	hair dryer	towel	cd case	fireplace	alarm clock	desk	folded chair	ceiling
toilet seat cover dispenser	water bottle	door	closet rod	mini fridge	music stand	bathroom stall	storage bin	piano
furniture	purse	clothes	range hood	water cooler	storage bin	speaker	curtain	closet
cart	vent	whiteboard	projector screen	water pitcher	music stand	keyboard piano	folded chair	counter
storage container	water pitcher	bed	divider	pillar	storage bin	clothes dryer	storage bin	bench
tissue box	bowl	bathroom counter	whiteboard	ledge	alarm clock	headphones	curtain	ceiling
crate	floor	case of water bottles	bed	fireplace	music stand	toilet paper dispenser	shower door	piano
dish rack	paper bag	coffee kettle	bathroom counter	mini fridge	storage bin	coffee table	curtain	closet
range hood	alarm clock	shower head	case of water bottles	water cooler	music stand	desk	folded chair	counter
dustpan	laundry detergent	case of water bottles	coffee kettle	water pitcher	storage bin	bathroom stall	storage bin	bench
handicap bar	object	fire alarm	shower head	pillar	alarm clock	speaker	curtain	ceiling
mailbox	ceiling light	power strip	case of water bottles	ledge	music stand	keyboard piano	folded chair	piano
music stand	dumbbell	calendar	coffee kettle	fire alarm	storage bin	clothes dryer	storage bin	closet
bathroom counter	tube	posters	shower head	water cooler	alarm clock	headphones	curtain	counter
bathroom vanity	cd case	power strip	case of water bottles	water pitcher	music stand	toilet paper dispenser	shower door	bench
laundry hamper	coffee kettle	calendar	fire alarm	pillars	storage bin	coffee table	curtain	ceiling
trash bin	shower head	posters	power strip	ledge	alarm clock	desk	folded chair	piano
keyboard piano	case of water bottles	posters	calendar	fire alarm	storage bin	bathroom stall	storage bin	closet
folded chair	fire alarm	posters	posters	pillars	alarm clock	speaker	curtain	counter
luggage	power strip	potted plant	posters	ledge	storage bin	keyboard piano	folded chair	bench
mattress	calendar	potted plant	potted plant	fire alarm	alarm clock	clothes dryer	storage bin	ceiling
	posters	potted plant	mattress	pillars	storage bin	headphones	curtain	piano

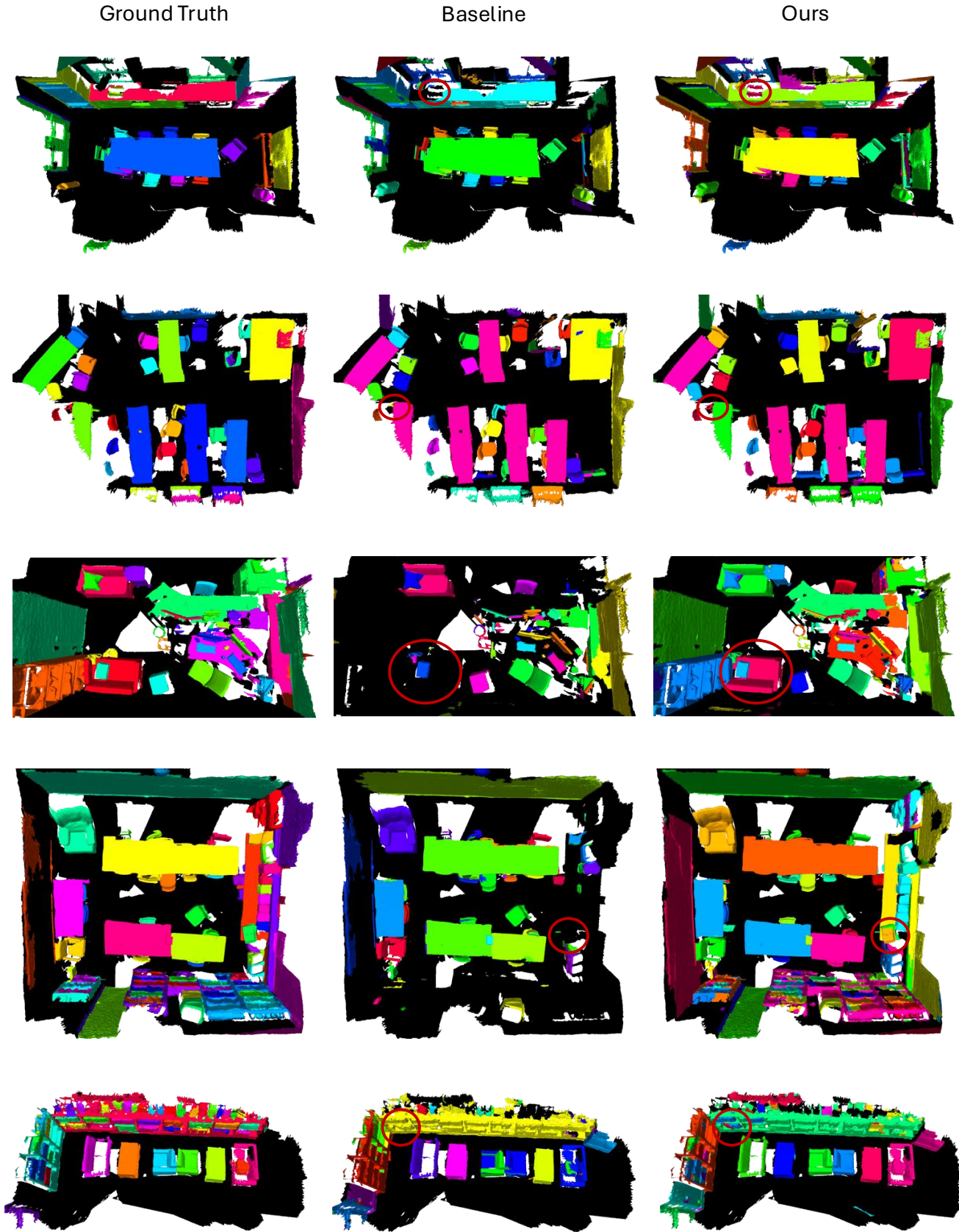


Figure 4. Qualitative comparison of ground truth, the baseline method, and our proposed framework on the Split_A evaluation after learning all tasks.

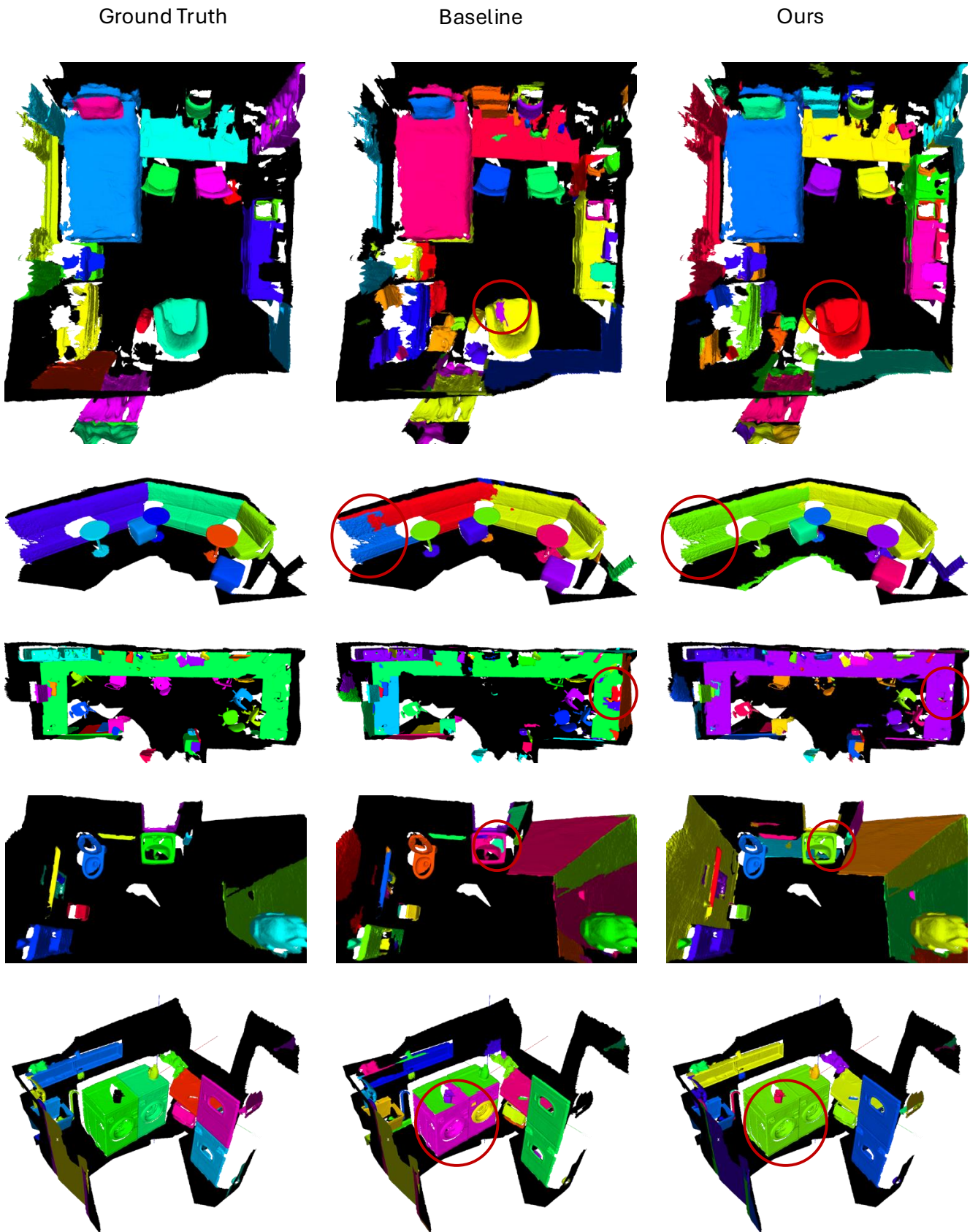


Figure 5. Qualitative comparison of ground truth, the baseline method, and our proposed framework on the Split_B evaluation after learning all tasks.

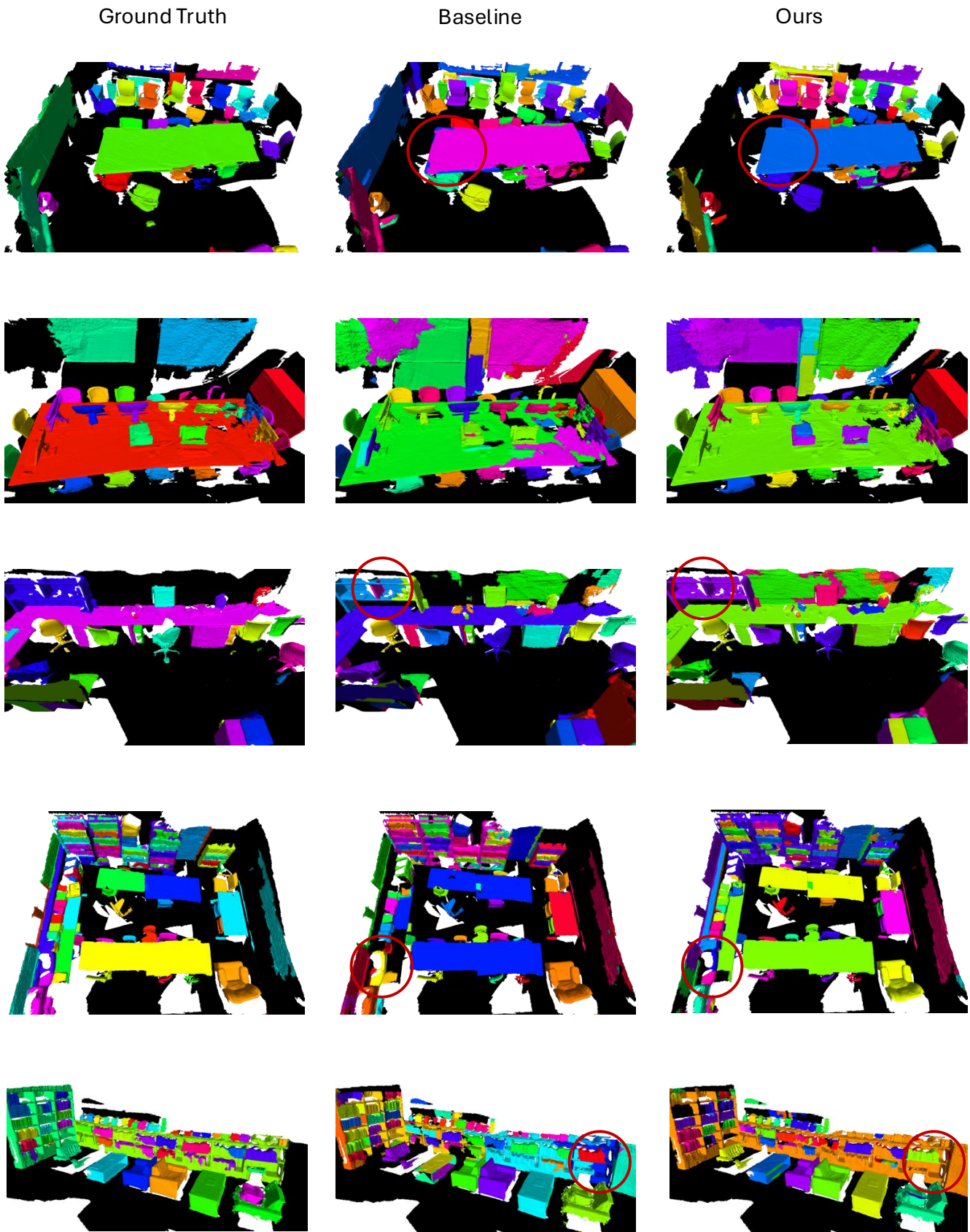


Figure 6. Qualitative comparison of ground truth, the baseline method, and our proposed framework on the Split_C evaluation after learning all tasks.